Quasifree $(e, e'p)$ Reactions and Proton Propagation in Nuclei

D. Abbott,[21] A. Ahmidouch,[7] Ts. A. Amatuni,[24] C. Armstrong,[23] J. Arrington,[2] K. A. Assamagan,[6] K. Bailey,[1]
O. K. Baker,[21,6] S. Barrow,[17] K. Beard,[6] D. Beatty,[17] S. Beedoe,[13] E. Beise,[11] E. Belz,[4] C. Bochna,[9] H. Breuer,[11]
E. E. W. Bruins,[10] R. Carlini,[21] J. Cha,[6] N. Chant,[11] C. Cothran,[22] W. J. Cummings,[1] S. Danagoulian,[13] D. Day,[22]
D. DeSchepper,[10] J.-E. Ducret,[20] F. Duncan,[11] J. Dunne,[21] D. Dutta,[14] T. Eden,[6] R. Ent,[21] H. T. Fortune,[17] V. Frolov,[18]
D. F. Geesaman,[1] H. Gao,[9] R. Gilman,[21,19] P. Guèye,[6] J. O. Hansen,[1] W. Hinton,[6] R. J. Holt,[9] C. Jackson,[13]
H. E. Jackson,[1] C. E. Jones,[1] S. Kaufman,[1] J. J. Kelly,[11] C. Keppel,[21,6] M. Khandaker,[12] W. Kim,[8] E. Kinney,[4]
A. Klein,[16] D. Koltenuk,[17] L. Kramer,[10] W. Lorenzon,[17] K. McFarlane,[12] D. J. Mack,[21] R. Madey,[6,7] P. Markowitz,[5]
J. Martin,[10] A. Mateos,[10] D. Meekins,[21] M. A. Miller,[9] R. Milner,[10] J. Mitchell,[21] R. Mohring,[11] H. Mkrtchyan,[24]
A. M. Nathan,[9] G. Niculescu,[6] I. Niculescu,[6] T. G. O'Neill,[1] D. Potterveld,[1] J. W. Price,[18] J. Reinhold,[1] C. Salgado,[12]
J. P. Schiffer,[1] R. E. Segel,[14] P. Stoler,[18] R. Suleiman,[7] V. Tadevosyan,[24] L. Tang,[21,6] B. Terburg,[9] D. van Westrum,[4]
Pat Welch,[15] C. Williamson,[10] S. Wood,[21] C. Yan,[21] Jae-Choon Yang,[3] J. Yu,[17] B. Zeidman,[1]
W. Zhao,[10] and B. Zihlmann[22]

[1]*Argonne National Laboratory, Argonne, Illinois 60439*
[2]*California Institute of Technology, Pasadena, California 91125*
[3]*Chungnam National University, Taejon 305-764 Korea*
[4]*University of Colorado, Boulder, Colorado 80309*
[5]*Florida International University, University Park, Florida 33199*
[6]*Hampton University, Hampton, Virginia 23668*
[7]*Kent State University, Kent, Ohio 44242*
[8]*Kyungpook National University, Taegu, South Korea*
[9]*University of Illinois, Urbana-Champaign, Illinois 61801*
[10]*Massachusetts Institute of Technology, Cambridge, Massachusetts 02139*
[11]*University of Maryland, College Park, Maryland 20742*
[12]*Norfolk State University, Norfolk, Virginia 23504*
[13]*North Carolina A. & T. State University, Greensboro, North Carolina 27411*
[14]*Northwestern University, Evanston, Illinois 60201*
[15]*Oregon State University, Corvallis, Oregon 97331*
[16]*Old Dominion University, Norfolk, Virginia 23529*
[17]*University of Pennsylvania, Philadelphia, Pennsylvania 19104*
[18]*Rensselaer Polytechnic Institute, Troy, New York 12180*
[19]*Rutgers University, New Brunswick, New Jersey 08903*
[20]*Centre d'Etudes Nucleaires de Saclay, Gif-sur-Yvette, France*
[21]*Thomas Jefferson National Accelerator Facility, Newport News, Virginia 23606*
[22]*University of Virginia, Charlottesville, Virginia 22901*
[23]*William and Mary, Williamsburg, Virginia 23187*
[24]*Yerevan Physics Institute, Yerevan, Armenia*

The $(e, e'p)$ reaction was studied on targets of C, Fe, and Au at momentum transfers squared Q^2 of 0.6, 1.3, 1.8, and 3.3 GeV^2 in a region of kinematics dominated by quasifree electron-proton scattering. Missing energy and missing momentum distributions are reasonably well described by plane wave impulse approximation calculations with Q^2 and A dependent corrections that measure the attenuation of the final state protons. [S0031-9007(98)06279-6]

The $(e, e'p)$ reaction with nearly free electron-proton kinematics (quasifree) has proven to be a valuable tool to study the propagation of nucleons in the nuclear medium [1–3]. The relatively weak interaction of the electron with the nucleus allows the electrons to penetrate the nuclear interior and knock out protons. These studies complement nucleon-induced measurements of proton propagation in nuclei which give more emphasis to the nuclear surface. This paper reports the first results of a systematic study of

the quasifree knockout of protons of 300–1800 MeV kinetic energy from carbon, iron, and gold targets. This energy range includes the minimum of the nucleon-nucleon (N-N) total cross section, the rapid rise in this cross section with energy above the pion production threshold, and extends to the long plateau in the energy dependence of the N-N total cross section. These features of the N-N interaction would be expected to be reflected in the energy dependence of attenuation of protons as they pass

through the nucleus but many body effects, including Pauli blocking, nonlocality, and correlations in the nuclear wave functions, can play an essential role in modifying this expectation (See Refs. [4–6], and references therein). The quasifree region is roughly defined by proton kinetic energies $T_p \sim Q^2/2M_p$ and outgoing proton momenta, $\vec{p}'$, close to $\vec{q} + \vec{p}_i$ where $\vec{q}$ is the electron three momentum transfer, Q^2 is the absolute value of the electron four momentum transfer squared, M_p is the proton mass, and $\vec{p}_i$ is a typical three momentum of the initial struck nucleon with $|\vec{p}_i|$ less than the Fermi momentum. (The convention $c = 1$ is used throughout this paper.) In comparison to previous experiments, the superb cw time structure and longitudinal emittance of the beam at the Thomas Jefferson National Accelerator Facility (Jefferson Lab) made possible measurements of much higher statistical and systematic precision and allowed a more complete coverage of the final state phase space.

This experiment was the first experiment to receive the beam at Jefferson Lab and utilized 100% duty factor electron beams of 2.45 and 3.25 GeV incident energies and currents of 10 to 50 μA. The electron beam current was monitored to 1% accuracy by three resonant cavities and a parametric transformer monitor. The targets were solid foils of C (230 mg/cm^2), Fe (310 mg/cm^2), and Au (196 mg/cm^2), with the thicknesses determined to 0.2%. For $Q^2 < 3$ GeV^2, electrons were detected in the Hall C high momentum spectrometer (HMS, momentum acceptance $\frac{\Delta p}{p} = \pm 10\%$, solid angle $\Delta\Omega = 7.0$ msr) and protons were detected in the short orbit spectrometer (SOS, $\frac{\Delta p}{p} = \pm 20\%$, $\Delta\Omega = 7.5$ msr). At $Q^2 = 3.3$ GeV^2, electrons were detected in the SOS and protons in the HMS. The kinematics of the measurements are given in Table I.

The solid angle of each spectrometer was defined by a 2-in. thick tungsten collimator. The detectors in the two spectrometers were quite similar. Four segmented planes of plastic scintillator were used to form the trigger and to provide time of flight information. Two 6-

TABLE I. Kinematics of the measurements. The proton angle shown in bold face includes free e-p kinematics.

Average T_p (MeV)	Electron energy (GeV)	Q^2 (GeV^2)	Electron θ_{LAB} (degrees)	Proton θ_{LAB} (degrees)
350	2.445	0.6	20.5	35.4, 39.4, 43.4, 47.4, 51.4, **55.4**, 59.4, 63.4, 67.4, 71.4, 75.4
700	2.445	1.3	32.0	31.0, 35.0, 39.0, **43.0**, 47.0, 51.0, 55.0
970	3.245	1.8	28.6	33.5, 37.5, **40.5**, 44.5, 48.5, 52.5
1800	3.245	3.3	50.0	**25.1**, 27.6, 30.1

plane drift chambers measured the particle trajectories. The tracking efficiency was monitored to 1%. Typical resolutions in momenta were 0.2% and in target angles were 0.8 (7.0) mr horizontal by 1.2 (0.5) mr vertical in the HMS (SOS). Additional particle identification was provided by segmented Pb-glass shower arrays and gas threshold Čerenkov counters. The corrections for particle loss via interactions with material in the spectrometers and detectors were also determined to 1%.

Electron-proton coincidence events and prescaled electron singles events were recorded in every run. Since the electron spectrometer was kept fixed at each Q^2, the electron singles yield provides a continuous monitor of the product of luminosity and electron reconstruction efficiency. Run-to-run variations are usually much less than 2%. After corrections for the measured particle trajectories, the coincidence timing resolution was 0.5 ns (FWHM). The real to random coincidence rate with the nuclear targets was typically greater than 100 to 1 and in the worst case, with the protons detected 20° forward of $\vec{q}$, 7 to 1. The spectrometer acceptance is determined by the Monte Carlo simulation of the apparatus, discussed below, with an estimated uncertainty of 1.5%, due in part to the sensitivity to variations in the defined region of acceptance.

At each momentum transfer absolute cross sections were checked with electron singles and electron-proton coincidence measurements of e-p elastic scattering from a 4.21 ± 0.01 cm liquid hydrogen cell and a dummy cell for background measurements. The absolute normalization of the hydrogen cross sections agreed with Monte Carlo simulations of the detector acceptance to $\pm 1.5\%$ using the dipole proton electric form factor and the Gari-Krümpelmann parametrization of the proton magnetic form factor [7], comparable to the fluctuations between various measurements and parametrizations of e-p cross sections [8]. The agreement of the e-p elastic scattering singles and coincidence measurements is a stringent test of many aspects of the experimental procedure.

If the $(e, e'p)$ cross section were completely described by quasifree scattering from individual nucleons (assuming only one body hadronic currents), then each scattered electron corresponds to an outgoing proton propagating through the nucleus with kinematics defined by the electron kinematics and the initial momentum and energy of the struck nucleon in the nucleus. If final state interactions were negligible, the cross section would be described in the plane wave impulse approximation (PWIA) by

$$\frac{d^6\sigma}{dE'_e d\Omega_e d^3 p'} = \sigma_{ep} S(E_m, \vec{p}_i), \qquad (1)$$

where E'_e and Ω_e represent the energy and angles of the outgoing electron. The spectral function, $S(E_m, \vec{p}_i)$, is the probability of finding a proton with separation energy E_m and initial momentum $\vec{p}_i$, and σ_{ep} is the off-shell e-p

cross section. In this limit of no final state interactions, the detected electron and proton determine the kinematics of the initial struck proton given by

$$-\vec{p}_i = \vec{p}_m = (\vec{q} - \vec{p}'), \qquad (2)$$

$$E_m = \omega - T_p - T_{A-1}, \qquad (3)$$

in which ω is the electron energy transfer ($Q^2 = \vec{q}^{\,2} - \omega^2$), and T_{A-1} the kinetic energy of the recoiling $A - 1$ nucleons.

In reality the electron trajectory is modified by Coulomb scattering and radiative effects which are included in the simulation discussed below. The primary focus here is on the interaction of the proton with the residual nucleus. This experiment measures the flux of protons in the quasifree region which is taken to be $E_m < 80$ MeV and $|\vec{p}_i| < 300$ MeV. Interactions such as large angle nucleon-nucleon rescattering and inelastic pion production that dramatically change the energy or angle of the emerging nucleon result in attenuation of the accepted ejectile flux. This loss of flux is measured by an average nuclear transparency, T. Processes which make only small shifts in the kinematics of the outgoing proton, such as elastic proton-nucleus rescattering, low energy nuclear excitations of the residual nucleus, or small angle, low momentum transfer, N-N rescattering (which is constrained by Pauli blocking of the final nucleon states), cannot be separated kinematically from events that have no rescattering.

In this paper, the consistency of the data with calculations performed with the assumptions of a single nucleon mechanism and negligible contamination from rescattering processes serves as a test of the reaction mechanism. These assumptions will break down well away from the quasifree peak. At lower Q^2, significant differences have been observed between the yields for longitudinal and transverse virtual photons indicating the importance of multibody currents [9]. At higher Q^2 unseparated spectral functions of Refs. [2] and [3] appeared consistent with a single nucleon mechanism with radiative corrections. In future publications, the spectral functions extracted from each kinematics in the present experiment and a longitudinal-transverse separation of the cross sections at Q^2 of 0.6 and 1.8 GeV^2 will provide more powerful tests of the underlying reaction mechanisms, such as sensitivity to multibody currents.

The PWIA was used in a Monte Carlo simulation to calculate the expected yields under each set of kinematical conditions. The calculation used independent-particle spectral functions from Ref. [10]. Nucleon-nucleon correlations in realistic spectral functions are known to cause some of the single-particle strength to appear at larger E_m and $|\vec{p}_i|$ [11]. This effect was included by normalizing the single-particle strength to 0.90, 0.82, and 0.78 times Z, the number of protons, for C, Fe, and Au, respectively, following the procedure of Ref. [2]. The off-shell σ_{ep} was taken to be CC1 of Ref. [12]. The simulation included realistic

models of the experimental apparatus. Coulomb scattering of the electron was taken into account by including the effect of the Coulomb energy shift in the electron energies and the effective three momentum transfer correcting σ_{ep} and $\vec{p}_i$ following the prescription of Ref. [13]. The maximum correction, for Au, increases the calculated cross section by 5%. Radiative effects were included based on the underlying electromagnetic cross sections [10] to calculate distributions of events to compare with the experimental results. The estimated error on this procedure is 2%. Figure 1 shows the experimental missing energy distributions for carbon at the conjugate angle and the results of the simulation. The agreement at large E_m indicates essentially that all of this strength can be attributed to radiative effects and there is no evidence of significant rescattering contributions at this angle. Small differences in shape can be seen indicating the choices of single-particle energies and widths and instrumental resolutions are not yet optimized, but the results given below are not sensitive to small changes in these parameters. For each proton angle, T_θ was determined by

$$T_\theta = \frac{\int_V d^3 p_i dE_m N_{\exp}(E_m, \vec{p}_i)}{\int_V d^3 p_i dE_m N_{\mathrm{PWIA}}(E_m, \vec{p}_i)}, \qquad (4)$$

where V is the finite experimental phase-space volume (with $E_m < 80$ MeV and $|\vec{p}_i| < 300$ MeV), and $N_{\exp}(E_m, \vec{p}_i)$ and $N_{\mathrm{PWIA}}(E_m, \vec{p}_i)$ are the normalized yields of the measurement and simulation, respectively. Figure 2 shows the angular dependence relative to the conjugate angle of the normalized yield and T_θ for iron at each Q^2. There is evidence at the extreme angles of
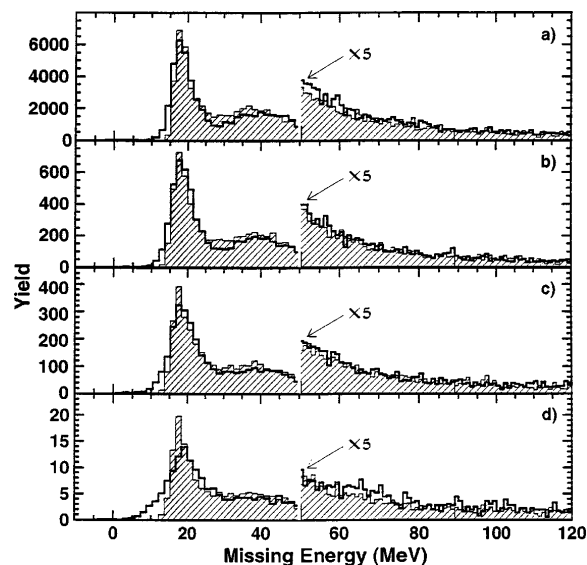

FIG. 1. Missing energy spectra for $C(e, e'p)$ reactions at the angle corresponding to free e-p kinematics for (a) $Q^2 = 0.6$, (b) $Q^2 = 1.3$, (c) $Q^2 = 1.8$, and (d) $Q^2 = 3.3$ GeV^2. The shaded histograms are the result of the simulation discussed in the text. The region from 0 to 80 MeV is integrated to define the quasifree yield.
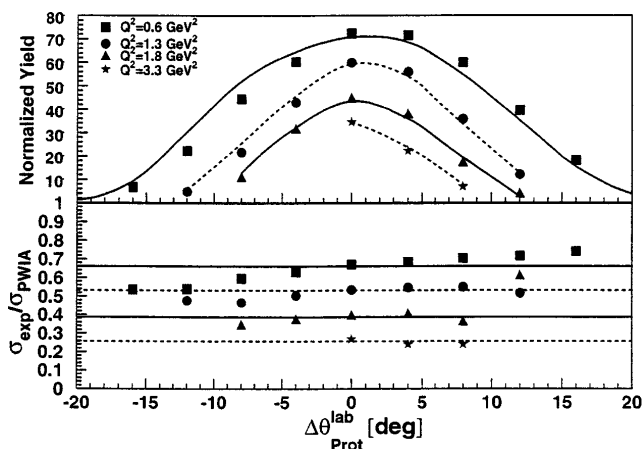
FIG. 2. (Upper panel) experimental $(e, e'p)$ coincidence yields vs the difference between the proton spectrometer lab angle and the conjugate angle for data from Fe at each momentum transfer. Scale factors of 0.21, 1.6, 2.25, and 35 have been applied at $Q^2 = 0.6$, 1.3, 1.8, and 3.3, respectively. (Lower panel) T_θ as a function of proton angle. The results are displaced by $+0.2$, $+0.1$, 0.0, and -0.15 for $Q^2 = 0.6$, 1.3, 1.8, and 3.3, respectively. In each case statistical errors of the data are smaller than the plotting symbols. The curves in each panel are simulations of the yield based on the model described in the text and normalized by a single T factor for each Q^2.

other reaction mechanisms such as proton rescattering or $(e, e'n)$ followed by (n, p) charge exchange, but the yield is weak compared to the dominant quasifree strength. At the lower Q^2 values, Fig. 2 shows evidence of a left-right asymmetry in T_θ indicating the presence of a longitudinal-transverse interference term in the cross section, roughly 20% beyond that of the off-shell σ_{ep} cross section. This asymmetry decreases as the momentum transfer increases supporting our analysis at the highest Q^2 and the analysis of Refs. [2,3] where data are generally available only at proton angles greater than or equal to the conjugate angle. It does raise a concern for the lowest Q^2 measurements of Ref. [1]. Similar asymmetries are observed on all three targets. The yields on each target for all angles were summed to determine the overall ratio of data to simulation and a single value of T for each Q^2. The lines in Fig. 2 represent the simulations multiplied by these T values.

The systematic error in T from experimental uncertainties and the radiative correction procedure is 3.2%. Choosing the de Forest CC2 prescription [12] for the off-shell cross section changes T by 1.5% with only $\pm 0.5\%$ variation with target and kinematics. The other dominant systematic errors in T result from the model dependence of the nuclear spectral function, especially the correlation corrections, and are estimated to range from 4% for C to 11% for Au. These do not affect the Q^2 dependence of the results on a single target but must be remembered in considering the A dependence. In Ref. [1] at lower Q^2, this uncertainty

could be reduced by considering the ratio of coincidence to singles cross sections where many of the model dependent effects cancel out. This procedure cannot be followed at higher momentum transfer because the singles spectra begin to receive significant nucleon inelastic contributions which are not included in the coincidence yield.

Figure 3 presents the measured values of T from this and previous work as a function of Q^2. The errors on the present work include the experimental systematic errors, but not the model dependence of the simulations. The present results are consistent with the previous work and are of substantially higher precision. Little evidence of momentum transfer or final-state proton energy dependence can be seen above Q^2 of 1.8 GeV^2. The dashed curves from $0.3 < Q^2 < 1.3$ GeV^2 are distorted wave impulse approximation calculations of Kelly [4] using a density dependent empirical effective interaction, of Ref. [4], fit to inelastic scattering data that successfully describe proton-nucleus absorption cross sections up to $T_p = 700$ MeV. These calculations provide a good description of the carbon results but underpredict the transparency on the heavier nuclei. The solid curves from $0.2 < Q^2 < 8$ GeV^2 are preliminary results of correlated Glauber calculations [5] including rescattering through third order. These calculations agree well with Monte Carlo calculations [6] for ^{16}O and ^{40}Ca for which the two methods have been compared. The Glauber calculations describe the carbon results at higher Q^2 well, but also underpredict the transparency for the heavier nuclei,
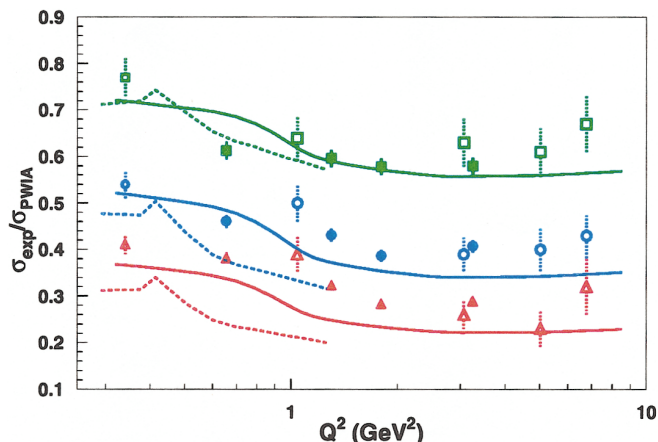

FIG. 3(color). $T = \sigma_{\exp}/\sigma_{\mathrm{PWIA}}$ for $(e, e'p)$ quasielastic scattering from C (green), Fe (blue), and Au (red) targets as a function of the momentum transfer Q^2. Data from the present work are the solid squares, circles, and triangles, respectively. Data from NE-18 (open squares, circles, and triangles) are from Ref. [2] and data from Bates at the lowest Q^2 on C, Ni, and Ta targets (small open symbols) are from Ref. [1]. The errors from the present work, $\pm 3.2\%$, and the NE-18 errors shown here do not include model dependent systematic errors on the simulations. The dashed curves from $0.3 < Q^2 < 1.3$ GeV^2 are DWIA calculations [4] and the solid curves from $0.2 < Q^2 < 8$ GeV^2 are Glauber calculations [5].

though by a lesser amount, and show more energy dependence at lower Q^2 than the present data. The calculated energy dependence is a partial reflection of the minimum in the N-N total cross section at $T_p \sim 500$ MeV. For carbon our results are almost independent of T_p down to 350 MeV. The energy dependence gradually changes on the heavier targets to a shape similar to the Glauber calculation on gold. Part of the discrepancy in the A dependence of the calculations could be attributed to the uncertainty in the correlation corrections.

In summary we have reported precise measurements of the nuclear dependence of quasifree $(e, e'p)$ reactions and extracted the energy dependence of the macroscopic attenuation of the final state protons. The results on carbon do not reveal a significant increase in the nuclear attenuation in the energy range where the N-N total cross sections increase significantly as pion production begins to dominate. At the higher Q^2 ($T_p \sim 1$ GeV) little energy dependence is observed as predicted by the Glauber calculations. If the energy dependence of the reaction model is under control in this regime, these data place significant limits on possible changes of the proton magnetic form factor in the nuclear medium or the onset of additional interesting mechanisms such as color transparency.

[1] G. Garino *et al.,* Phys. Rev. C **45**, 780 (1992).
[2] T. G. O'Neill *et al.,* Phys. Lett. B **351**, 87 (1995).
[3] N. C. R. Makins *et al.,* Phys. Rev. Lett. **72**, 1986 (1994).
[4] J. J. Kelly, Phys. Rev. C **54**, 2547 (1996).
[5] H. Gao, V. R. Pandharipande, and S. C. Pieper (private communication); V. R. Pandharipande and S. C. Pieper, Phys. Rev. C **45**, 791 (1992).
[6] H. Gao, R. J. Holt, and V. R. Pandharipande, Phys. Rev. C **54**, 2779 (1996).
[7] M. Gari and W. Krümpelmann, Z. Phys. A **322**, 689 (1985).
[8] R. C. Walker *et al.,* Phys. Rev. D **49**, 5671 (1994).
[9] P. E. Ulmer *et al.,* Phys. Rev. Lett. **59**, 2259 (1987).
[10] T. G. O'Neill, Ph.D. thesis, California Institute of Technology, 1994 (unpublished); N. C. R. Makins, Ph.D. thesis, Massachusetts Institute of Technology, 1994 (unpublished).
[11] For example, see V. R. Pandharipande, I. Sick, and P. K. A. De Witt Huberts, Rev. Mod. Phys. **69**, 981 (1997).
[12] T. de Forest, Nucl. Phys. **A392**, 232 (1983).
[13] Y. Jin, H. P. Blok, and L. Lapikas, Phys. Rev. C **48**, R964 (1993).